DET NORSKE VIDENSKAPS-AKADEMI I OSLO

GEOFYSISKE PUBLIKASJONER
GEOPHYSICA NORVEGICA

Vol. XXVI. No. 11 December 1966

LAWRENCE H. LARSEN

Flow over obstacles of finite amplitude

OSLO 1966
UNIVERSITETSFORLAGET

GEOFYSISKE PUBLIKASJONER
GEOPHYSICA NORWEGICA
VOL. XXVI. NO. 11

FLOW OVER OBSTACLES OF FINITE AMPLITUDE

By Lawrence H. Larsen
University of Oslo, Institute of Geophysics

FREMLAGT I VIDENSKAPS-AKADEMIETS MØTE DEN 16DE SEPTEMBER 1966 AV ELIASSEN

Summary. This work deals with the flow of a perfect fluid over an isolated barrier. Of interest is the time development of the free surface for an impulsively started obstacle and the analysis for a steady flow about finite amplitude barriers. We show how for some obstacles no steady shock free flow will develop from the initial value problem. In these cases upstream blocking occurs altering the basic flow state. By including the non-linearities in a lee wave theory the study of lee waves is made compatible with the actual experimental evidence. This is contrasted with the linear theory which predicts lee-waves for all subcritical flows.

1. Introduction. Infinitesimal amplitude approaches to the description of the flow of a homogeneous or non-homogeneous fluid over an isolated barrier invariably show the existence of lee waves whenever standing free oscillations may occur. Such is not the case with a flow of finite amplitude as no steady flow about an arbitrarily high obstacle need exist even though infinitesimal standing oscillations are possible. Long (1954) has derived general criteria for the existence of a steady flow regime in one — and two — layered fluid systems. Finite amplitude models of certain stratified fluids have been shown by Long (1955) and Yih (1965) to also have a critical obstacle height above which no steady flow exists. They have established the criterion that if the obstacle is larger in amplitude than the height of the lowest nodal surface of the free oscillations then no steady solution exists.

This result of Long and Yih has been shown only for stratified fluid models which are described by a linear equation. Such as may be derived if we assume an incompressible fluid whose kinetic energy far upstream of the barrier is independent of altitude. In such flows no energy is fed into waves by shear in the basic flow. For an adiabatic fluid or for more general incompressible models such criteria have not been obtained. It is possible that the criteria differ in these more general models.

In this paper we discuss the flow of a perfect fluid with a free surface about a submerged barrier. The flow is examined first by numerically integrating a hydrostatic

model for an initial value problem and second by studying the formation of wave trains in a non-linear steady flow example. Before proceeding with the analytics it is worthwhile to examine the critical features of experimental observations. These experiments are reported by LONG (1954) and the reader is referred to his article for complete details.

The experiment consisted of pulling at a constant speed an obstacle along the bottom of a long narrow channel containing water. Initially both the fluid and the obstacle were at rest. The obstacle extended completely across the channel and was of gentle shape to minimize boundary layer effects. In the following the obstacle speed, c, is given in terms of the Froude number, $F^2=c^2/gH$, where g is gravity and H the initial fluid depth. The obstacle amplitude is measured in fractions of the initial fluid depth.

Long observed that for very small Froude numbers and after transient disturbances had propagated away from the obstacle the free surface was only slightly depressed over the obstacle. As the Froude number was increased the depression of the free surface over the obstacle deepened. Further increases in Froude number, for sufficiently small obstacles, led to the generation of lee waves behind the obstacle. The waves being stationary relative to the obstacle. However, for a given obstacle there existed a critical Froude number above which the transient disturbances ceased to propagate free of the obstacle, but instead developed into hydraulic jumps. For all obstacles this critical Froude numbers is less than unity.

For very high Froude numbers the transient disturbances were left behind the obstacle and the fluid crossed the obstacle maintaining a constant fluid depth. That is, the free surface followed the obstacle. As the Froude number was reduced the fluid continued to follow the obstacle, but at an increased amplitude. This amplification of the obstacle shape continued until some critical Froude number — greater than unity — was reached where a shock free flow no longer existed as an asymptotic state.

The cited experimental evidence shows that by far the most important feature of the flow is the development of hydraulic jumps. Thus it is necessary that any attempt at an analytical description of the time dependent problem involve non-linearities which permit waves to develop into breakers. If we assume the flow is absolutely hydrostatic, this requirement is met as it is known that any finite amplitude hydrostatic wave of elevation must steepen in front as it progresses.

Section 3 of this paper is devoted to the hydrostatic model. The equations are integrated numerically for the initial value problem of an impulsively started obstacle. The integrations show how a non-steady state evolves when transient disturbances cannot propagate away from the barrier quickly enough. Steady hydrostatic flows are also considered as they form the background for the lee wave problem discussed in section 4.

The possibility of wave trains may be introduced into a hydrostatic model if we permit some departure from a hydrostatic pressure field. FRIEDRICHS (1948), KELLER (1948), and WEHAUSEN and LAITONE (1960) have derived equations which are valid for long waves of small but finite amplitude. The leading terms in their expansion are the hydrostatic equations. The next term involves the curvature of the free surface.

In both of the derivations it is assumed that the second derivative of any quantity is at most of the order of magnitude of the quantity squared. With this assumption, which we shall call the solitary wave assumption, they expand in the amplitude of the disturbance retaining terms of first and second orders. Solitary and cnoidal waves are contained in this set of equations.

Such a restriction placed on a relationship between derivatives and amplitudes is not necessary. Accordingly we shall expand the equations of motion solely in terms of wave number, retaining fully the non-linearities. It might be argued that such an approach is in reality no more valid than the usual amplitude expansion for the solitary wave since disturbances of large amplitude tend to have sharpened crests. Consequently higher order wave numbers must be considered. This is true for free waves but near a barrier the amplitude of a disturbance may be large without sharpening, particularly so when the free surface is depressed over the obstacle. The consequences of making the solitary wave assumption are discussed. This type of approximation procedure can be generalized to non-homogeneous fluids and thus its consequences in this problem are of interest.

2. Development of the governing equations. We adopt a coordinate system with x in the horizontal direction and y in vertical direction. The corresponding fluid velocities are u and v. The fluid density is taken as unity and all quantities are nondimensionalized on H, the initial fluid depth, and g, gravity. Fo example, all velocities are measured as fractions of $(gH)^{\frac{1}{2}}$, i.e. $u=u_{\text{physical}}/(gH)^{\frac{1}{2}}$. The time, t, is measured in units of $(H/g)^{\frac{1}{2}}$.

Assuming irrotational motion of a perfect fluid, the Eulerian equations of motion are equivalent to Laplace's equation

$$\nabla^2\phi=0. \tag{2.1}$$

The velocity potential, ϕ, is defined as $u=-\phi_x$, $v=-\phi_y$. Subscripts are used to denote partial differentiation throughout this paper.

At the free surface $y=1+\eta(x,t)$ the fluid must obey the kinematic condition

$$\eta_t=-\phi_y+\eta_x\phi_x, \tag{2.2}$$

and the surface pressure condition

$$\eta=\phi_t-\tfrac{1}{2}(\phi_x^2+\phi_y^2). \tag{2.3}$$

We have taken the surface pressure to vanish and assumed that at some time the free surface displacement, η, vanishes.

At the obstacle and along the channel bottom the fluid must obey the kinematic condition

$$\phi_y=-s_t+\phi_x s_x, \tag{2.4}$$

where $y=s(x,t)$ is the shape of the lower boundary.

The most general solution, LAMB (1932), of (2.1) is

$$\phi=G_1(x,t)-\frac{y^2}{2!}G_{1xx}+\frac{y^4}{4!}G_{1xxxx}+\cdots+yG_{2x}(x,t)-\frac{y^3}{3!}G_{2xxx}+\frac{y^5}{5!}G_{2xxxxx}+\cdots \tag{2.5}$$

where G_1 and G_2 are arbitrary different functions of x and t. This series approach to long wave problems has been used successfully by LONG (1963) in his study of the development of solitary waves. Substituting (2.5) into the boundary conditions we obtain

$$\begin{aligned}\eta_t=&(1+\eta)G_{1xx}-\frac{(1+\eta)^3}{3!}G_{1xxxx}-G_{2x}+\frac{(1+\eta)^2}{2!}G_{2xxx}-\frac{(1+\eta)^4}{4!}G_{2xxxxx}\\&+\eta_x\left\{G_{1x}-\frac{(1+\eta)^2}{2!}G_{2xxx}+\frac{(1+\eta)^4}{4!}G_{1xxxxx}+(1+n)G_{2xx}-\frac{(1+\eta)^3}{3!}G_{2xxxx}\right\}+\cdots,\end{aligned} \tag{2.6}$$

$$\begin{aligned}\eta=&G_{1t}-\frac{(1+\eta)^2}{2!}G_{1xxt}+\frac{(1+\eta)^4}{4!}G_{1xxxxt}+(1+\eta)G_{2xt}-\frac{(1+\eta)}{3!}G_{2xxxt}+\frac{(1+\eta)^5}{5!}G_{2xxxxxt}\\&-\tfrac{1}{2}\left\{G_{1x}-\frac{(1+\eta)^2}{2!}G_{1xxx}+\frac{(1+\eta)^4}{4!}G_{1xxxxx}+(1+\eta)G_{2xx}-\frac{(1+\eta)^3}{3!}G_{2xxxx}\right\}^2\\&-\tfrac{1}{2}\left\{-(1+\eta)G_{1xx}+\frac{(1+\eta)^3}{3!}G_{1xxxx}+G_{2x}-\frac{(1+\eta)^2}{2!}G_{2xxx}\right\}^2+\cdots,\end{aligned} \tag{2.7}$$

and

$$\begin{aligned}G_{2x}=&\frac{s^2}{2!}G_{2xxx}-\frac{s^4}{4!}G_{2xxxxx}+sG_{1xx}-\frac{s^3}{3!}G_{1xxxx}-s_t+s_x\left\{G_{1x}-\frac{s^2}{2!}G_{1xxx}\right.\\&\left.+\frac{s^4}{4!}G_{1xxxxx}+sG_{2xx}-\frac{s^3}{3!}G_{2xxxx}\right\}+\cdots.\end{aligned} \tag{2.8}$$

Differentiating (2.7) with respect to x and introducing $U\equiv -G_{1x}$ into the equations we find after some rearrangement

$$\begin{aligned}\eta_t=&-(1+\eta)U_x-\eta_xU-G_{2x}+\left\{\frac{(1+\eta)^3}{3!}U_{xx}+\frac{(1+\eta)^2}{2!}G_{2xx}\right\}_x\\&+\left\{-\frac{(1+\eta)^5}{5!}U_{xxxx}-\frac{(1+\eta)^4}{4!}G_{2xxxx}\right\}_x+\cdots\end{aligned} \tag{2.9}$$

$$U_t=-\eta_x-UU_x+\left\{\frac{(1+\eta)^2}{2!}U_{xt}+(1+\eta)G_{2xt}+\frac{(1+\eta)^2}{2!}UU_{xx}+(1+\eta)UG_{2xx}-\tfrac{1}{2}(1+\eta)^2U_x^2\right.$$

$$\left.-\tfrac{1}{2}G_{2x}^2-(1+\eta)U_xG_{2x}\right\}_x-\left\{\frac{(1+\eta)^4}{4!}U_{xxxt}+\frac{(1+\eta)^3}{3!}G_{2xxxt}+\frac{(1+\eta)^4}{4!}UU_{xxxx}+\frac{(1+\eta)^3}{3!}UG_{2xxxx}\right. \tag{2.10}$$

$$+\frac{(1+\eta)^4}{8}U_{xx}^2+\frac{(1+\eta)^2}{2!}G_{2xx}^2-\frac{(1+\eta)^4}{3!}U_xU_{xxx}-\frac{(1+\eta)^3}{3!}U_{xxx}G_{2x}-\frac{(1+\eta)^3}{2!}U_xG_{2xxx}$$

$$\left.-\frac{(1+\eta)^2}{2!}G_{2x}G_{2xxx}\right\}_x+\cdots,$$

and

$$G_{2x}=-s_t-Us_x-sU_x+\left\{\frac{s^3}{3!}U_{xx}+\frac{s^2}{2!}G_{2xx}\right\}_x-\left\{\frac{s^5}{5!}U_{xxxx}+\frac{s^4}{4!}G_{2xxxx}\right\}_x+\cdots. \tag{2.11}$$

Physically U represents the fluid velocity at the bottom of a flat channel.

Now we assume that derivatives of higher order than three are negligible (equivalent to retaining the leading two terms in an expansion in wave-number) and we eliminate G_{2x} using (2.11). This yields the pair of equations

$$\eta_t=s_t-\left\{(1+\eta-s)U+\frac{(s^3-(1+\eta)^3)}{3!}U_{xx}+\frac{1}{2!}(s^2-(1+\eta)^2)G_x\right\}_x, \tag{2.12}$$

and

$$V_t=-\left\{\eta+\frac{U^2}{2}-\frac{(1+\eta)^2}{2}U_{xt}-(1+\eta)G_t-\frac{(1+\eta)^2}{2}UU_{xx}-(1+\eta)UG_x+\tfrac{1}{2}(1+\eta)^2U_x^2\right. \tag{2.13}$$

$$\left.+\tfrac{1}{2}G^2+(1+\eta)U_xG\right\}_x,$$

where

$$G\equiv-s_t-(Us)_x. \tag{2.14}$$

It is desirable to eliminate the time dependence on the right hand side of (2.13). This may be done by successively approximating for U_t. This yields

$$U_t=-\left\{\eta+\frac{U^2}{2}+\frac{(1+\eta)^2}{2}\eta_{xx}+(1+\eta)^2U_x^2-(1+\eta)G_t-(1+\eta)UG_x+\tfrac{1}{2}G^2+(1+\eta)U_xG\right\}_x. \tag{2.15}$$

Equations (2.12) and (2.15) are the governing equations whose solutions are considered in the remainder of this work. No assumption on the amplitude of the obstacle of free surface displacements has been made. The limitations of these equations are discussed in section 4.

3. A hydrostatic model.

3.0. Introductory remarks. This section contains three major subdivisions. In the first we discuss the types of solutions to be expected of a hydrostatic flow when the motion is steady. This section contains little new material but is included because the analysis forms the basis for the discussion on lee waves in section 4.

The second part of this section contains the numerical results of integrating the hydrostatic equations for an impulsively started obstacle. In the final section we discuss a method of approximating, in the non-steady region, the asymptotic solutions of the time dependent problem.

Retaining only first derivative terms in (2.12) and (2.15) we obtain the system

$$h_t = -(hU)_x \tag{3.1}$$

and

$$U_t = -\left(h+s+\frac{U^2}{2}\right)_x \tag{3.2}$$

where $h=1+\eta-s$ is the total fluid depth. Note that to this order of approximation the velocity, U, is uniform throughout the fluid depth.

3.1. Steady flows. In a coordinate system moving with the obstacle and for steady motion the time derivatives in (3.1) and (3.2) vanish. Integrating the steady forms of (3.1) and (3.2), we have the equations

$$hU=K_1, \tag{3.3}$$

and

$$h+\frac{U^2}{2}+s(x)=K_2, \tag{3.4}$$

where K_1 and K_2 are constants. The first equation, (3.3), is immediately recognizable as the continuity equation and the second, (3.4), as the energy equation.

If in the coordinate system moving with the obstacle we take the fluid to flow from right to left and assume that the upstream depth is unity, the constants K_1 and K_2 have the values $-F$ and $1+F^2/2$. The fluid is assumed to approach the obstacle at a Froude number F, and it is assumed that the obstacle vanishes in the upstream direction. Using these values for K_1 and K_2 and eliminating U between (3.3) and (3.4) we find

$$h^3-\left(1+\frac{F^2}{2}-s(x)\right)h^2+\frac{F^2}{2}=0. \tag{3.5}$$

The roots of this cubic determine the evolution of the free surface.

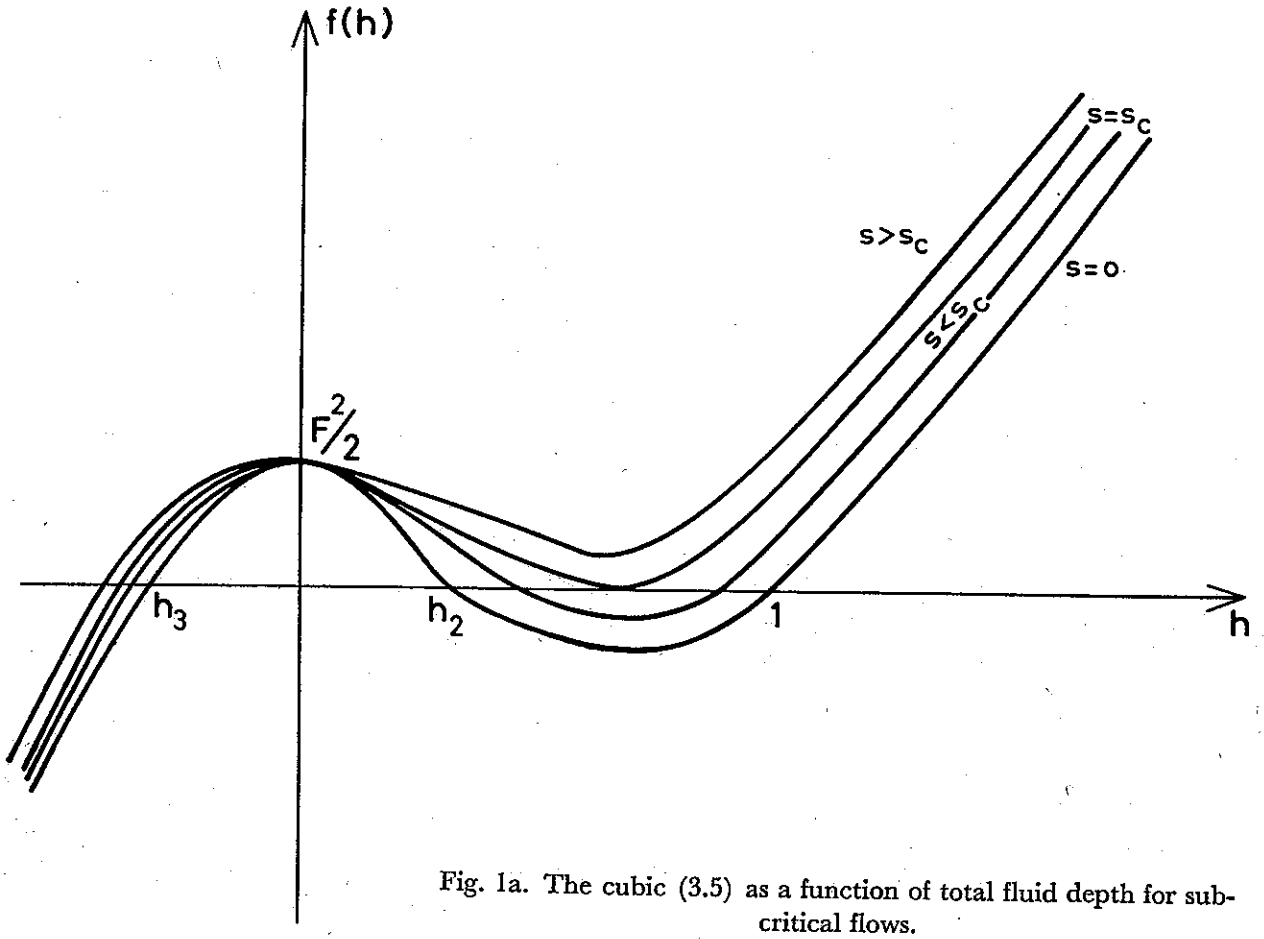

Fig. 1a. The cubic (3.5) as a function of total fluid depth for sub-critical flows.

When the obstacle, s, vanishes the cubic has the roots

$$h_1=1,$$
$$h_2=\frac{F^2}{4}+\tfrac{1}{4}(F^4+8F^2)^{\frac{1}{2}},$$
$$h_3=\frac{F^2}{4}-\tfrac{1}{4}(F^4+8F^2)^{\frac{1}{2}}. \tag{3.6}$$

The root h_1 corresponds to uniform flow. The root h_3 may be shown to be negative for all Froude numbers and is physically uninteresting. The root h_2 is greater than unity if $F>1$ and less than unity if $F<1$. It is well-known that for a given energy and volume flux two states of motion exist. Classical bore theory is a result of combining the two states of motion having equal momentum and volume fluxes. The root, h_2 corresponds to that alternate state having the same energy and volume flux as the basic flow of unit depth and Froude number, F. The momentum fluxes in the two states are different.

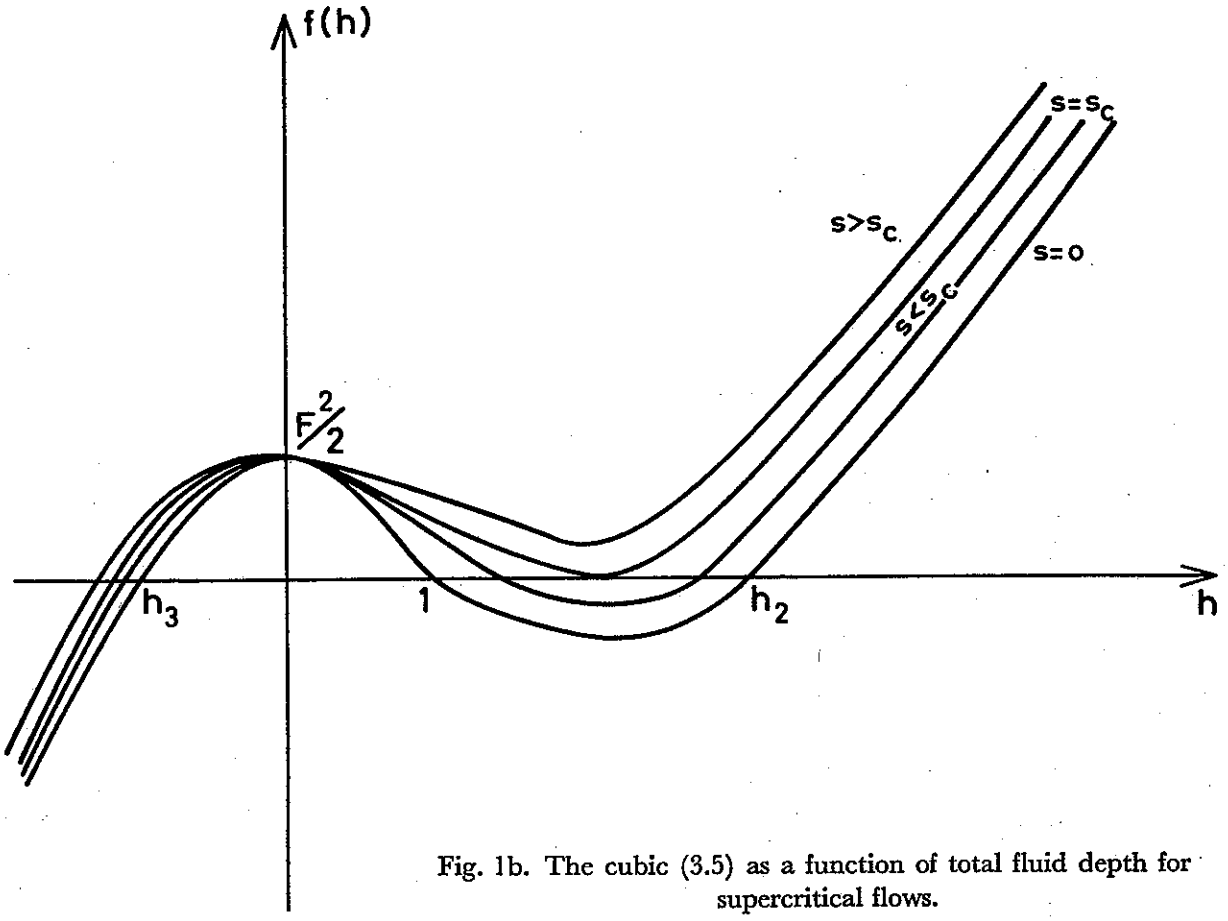

Fig. 1b. The cubic (3.5) as a function of total fluid depth for supercritical flows.

The behavior of the roots of (3.5) is shown in Figs. 1a and 1b. In these Figures the ordinate is the function $f(h) \equiv h_3 - (1 + F^2/2 - s)h^2 + F^2/2$. In Fig. 1a, $f(h)$ as a function of h is illustrated for F less than unity. No particular scale is used in the Figures.

The Figure illustrates that as the obstacle amplitude increases the total depth of the fluid decreases. A calculation of the roots of the cubic shows that in all cases the decrease in the fluid depth is greater than the obstacle amplitude. It follows that the free surface is depressed on crossing the obstacle. However a limit exists to maximum obstacle size, denoted by s_c, permissible if the flow is to be described by (3.5). For obstacles of amplitude greater than s_c no physically acceptable roots of the cubic exist.

In Fig. 1b, $f(h)$ is plotted as a function of h for F greater than unity.

From Fig. 1b we see that for supercritical Froude numbers the total depth of the fluid increases above the obstacle. It follows that the free surface is elevated above the obstacle. As in the subcritical case, a limit exists on the obstacle size if the cubic (3.5) is to have physically acceptable solutions. Note that the rise of the fluid over the obstacle in supercritical flow is much greater than the corresponding fall of the free surface in subcritical flow.

When the obstacle amplitude is greater than s_c the flow must be unsteady somewhere as no steady solution exist. Thus we have imposed an impossible flow problem by assigning the values $-F$ and $1+F^2/2$ to K_1 and K_2. Some alteration of the basic flow must occur before the fluid motion can be described by an equation of the form (3.5).

The dependence of the critical obstacle size on Froude number may easily be found as the critical point occurs when the cubic (3.5) has two equal roots. This condition is that F and s_c be related by

$$F^2-3F^{2/3}=2(s_c-1). \tag{3.7}$$

The corresponding roots are

$$\begin{aligned} h_1&=h_2=F^{2/3},\\ h_3&=-\tfrac{1}{2}F^{2/3}. \end{aligned} \tag{3.8}$$

At the obstacle maximum the local Froude number, F_l, is

$$F_l^2=\frac{U^2}{h}=\frac{F^2}{h^3}=1. \tag{3.9}$$

Thus the occurrence of multiple roots of $f(h)$ is equivalent to the flow having a local Froude number of unity at the obstacle crest.

Because hydraulic jumps can occur only if a fluid is forced to change from a supercritical to a subcritical state, the boundary of the steady flow regime should correspond to a local Froude number of unity at the obstacle crest. For if we consider a fixed obstacle and slowly begin to increase the Froude number from some small value, the local Froude number at the obstacle maximum will continually increase. This follows from (3.11) as h is observed to decrease. If F_l increases beyond unity then as the obstacle amplitude decreases on the lee side, the flow must change from supercritical to subcritical. The corresponding argument for supercritical flow begins with a high F_l slowly reducing it as the Froude number decreases. In both cases it is clear that an unsteady flow regime will result from too large an obstacle. Long (1954) derives (3.7) on the basis of the above argument. Equation (3.7) is shown in Fig. 2.

3.2. The initial value problem. In this study the fluid is assumed initially at rest and at $t=0$ an obstacle, $s(x,0)$, begins to move at a speed F along the channel bottom. The same smooth function $s(x,t)=A\,\mathrm{sech}^2(\frac{1}{2}(x-Ft))$ is used in all calculations. We report here the results for an obstacle of maximum amplitude 0.1. The factor of $\frac{1}{2}$ is included to give the obstacle a width of approximately 40 grid points. The distance between each grid point is 0.2 of the fluid depth. This allowed for a reasonable time range without excessive computer time.

For numerical purposes it was found convenient to use a modified form of (3.1)

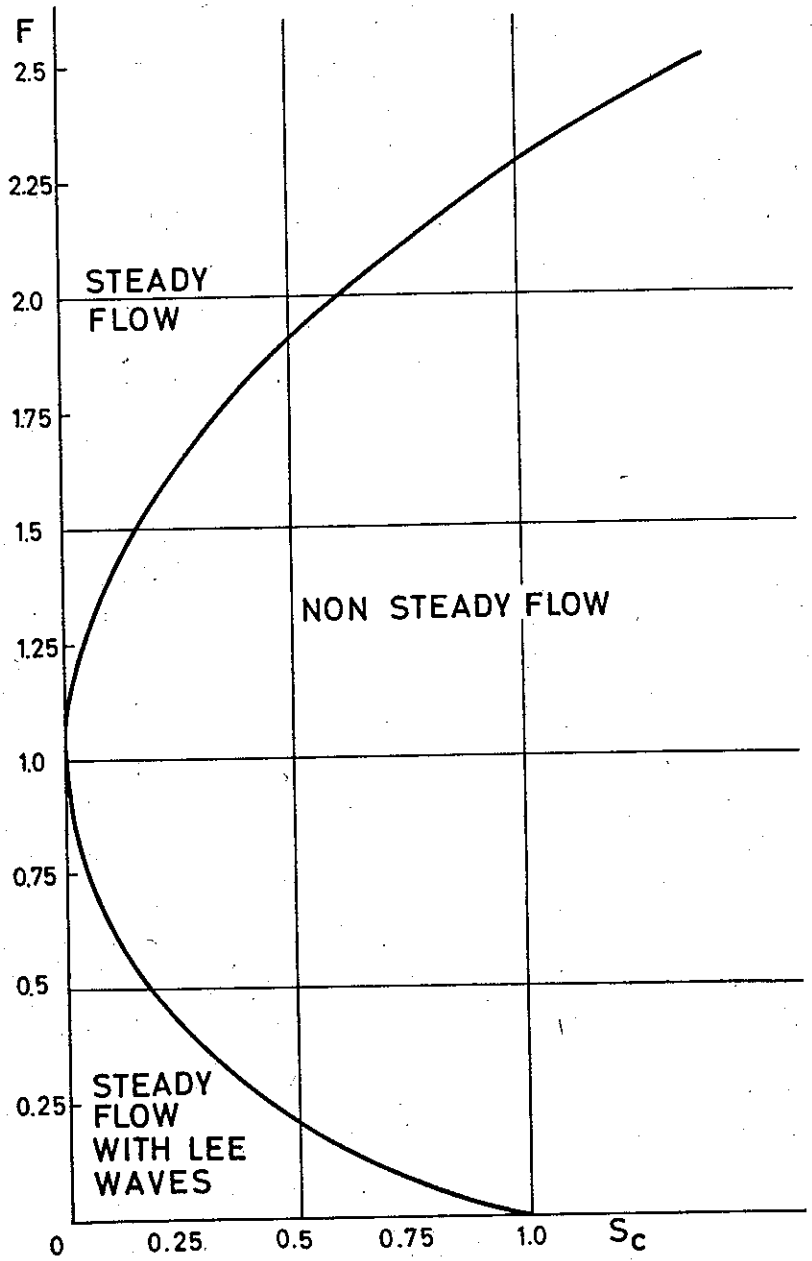

Fig. 2. Equation (3.7) illustrating regions of steady flows and non-steady flows.

and (3.2). Introducing $c^2 \equiv 1+\eta-s$, the speed of propagation of a free disturbance on a fluid of depth $1+\eta-s$, the equations are transformed to

$$c_t + Uc_x + \frac{c}{2}U_x = 0, \tag{3.10}$$

and

$$U_t + 2cc_x + UU_x = -s_x. \tag{3.11}$$

Apparently when this form of the equations is used, round off errors in the machine are less serious.

The computational procedure uses a three step calculation to evaluate quantities at time $t+\Delta t$ from the known quantities at time t. The method is illustrated by the equation

$$y_t = f(y). \tag{3.12}$$

We write

$$y_1\left(t+\frac{\Delta t}{2}\right) = y(t)+\frac{\Delta t}{2}f(y(t)), \tag{3.13}$$

and

$$y_2\left(t+\frac{\Delta t}{2}\right) = y(t)+\frac{\Delta}{4}\left\{f(y(t))+f\left[y_1\left(t+\frac{\Delta}{2}\right)\right]\right\}, \tag{3.14}$$

then

$$y(t+\Delta t) = y(t)+\Delta t f\left[y_2\left(t+\frac{\Delta}{2}\right)\right]. \tag{3.15}$$

In the actual computations a fixed region of space is defined through which the obstacle moves. For points interior to the region centered space differences are used and for boundary points one-sided derivatives are employed. For example, at interior points (3.10) is approximated by

$$c_t(x) = -\frac{U(x)}{2\Delta x}\{c(x+\Delta x)-c(x-\Delta x)\} \tag{3.16}$$

$$-\frac{c(x)}{4\Delta x}\{U(x+\Delta x)-U(x-\Delta x)\}.$$

No difficulties are encountered by disturbances reflecting from boundary points as they are observed to simply propagate out of the system. Initial tests of the method on a sinusoidal progressive wave — flat channel bottom — predicted the same time for breaking to occur as the analytic methods (STOKER 1957). The factor $\Delta t/\Delta x$ was taken as $\frac{1}{2}$ in all reported results. Decreases in the size of the time step led to identical results.

Solutions are shown for the development of steady flow (relative to the obstacle) in both subcritical and supercritical regions, F less than and greater than unity. Also shown are two non-steady flows, one subcritical and one supercritical. The free surface profiles are illustrated in Figs. 3—6. Dashed lines in the Figures indicate where the numerical results have been smoothed. Violent oscillations tended to develop in shock regions and these oscillations have been smoothed (free hand). The solid curves are drawn directly from the computer output.

The Figures encompass the entire computation region, 250 grid points, and show clearly the lack of interference from boundary points. The time axis in each figure is

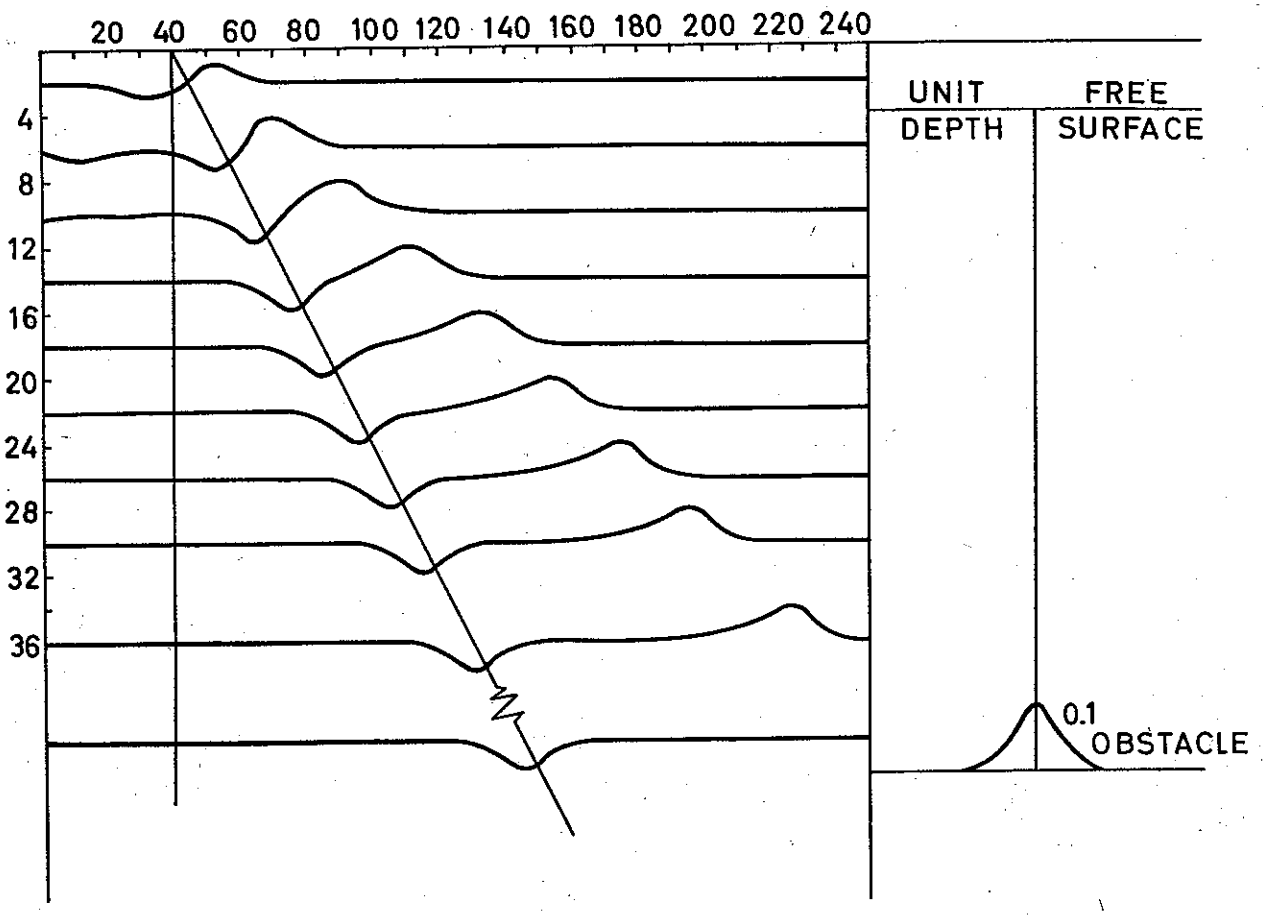

Fig. 3. Numerical results for a Froude number of 0.5 and an obstacle of amplitude 0.1. The grid spacing is 0.2.

positive downward and the slanting line shows the location of the obstacle maximum as a function of time. For comparison each Figure shows the obstacle and the initial fluid depth drawn in the same scale as the free surface profiles.

Fig. 3 contains the results for a subcritical regime of Froude number 0.5. As predicted by the analysis in section 3.1, steady solutions exist in this region and are indeed approached asymptotically in time. The steady solution, computed from the roots of (3.5), is the lowest curve in the Figure.

Initially it is seen that the free surface is pushed up in front of the obstacle and depressed in the lee. These initial depression and elevation waves then propagate away from the obstacle at their natural speeds. After propagating away only the depression wave over the obstacle remains. The initial wave of elevation has insufficient amplitude and fluid to develop into a breaker within the computation region.

In Fig. 4 the results for a Froude number of 1.5 are shown. The steady solution computed from (3.5) is shown at the bottom of the Figure. As in the subcritical case, initially the fluid is elevated in front of the obstacle and depressed in the wake. In this case both free waves are left behind the obstacle. The wave of elevation then steepens

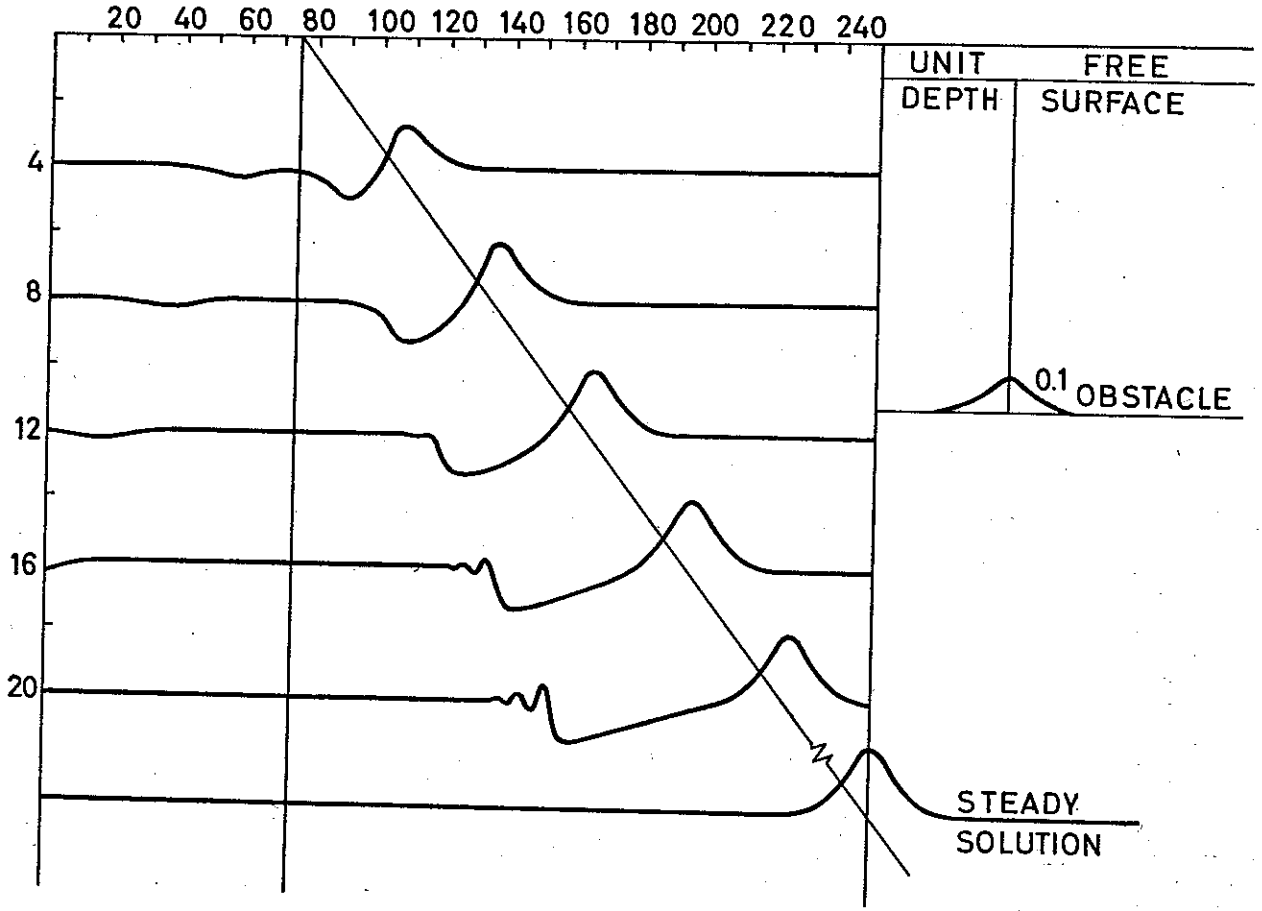

Fig. 4. Numerical results for a Froude number of 1.5 and an obstacle of amplitude 0.1. The grid spacing is 0.2.

and develops into a bore behind the obstacle. This bore however has insufficient amplitude to keep up with the obstacle. This phenomenon was observed by LONG (1954) in his experimental studies.

Flows for which a steady solution is not expected are shown in Figs. 5 and 6. Fig. 5 is for a Froude number of 0.7. As in the last two cases initially the free surface is elevated in front of the obstacle and depressed in the lee. Part of the initial depression wave is observed to propagate away behind the obstacle. The wave of elevation in front of the obstacle appears to be continually strengthened by fluid forced forward by the obstacle. This eventually leads to the upstream bore. In the lee the depression does not appear able to catch up with the obstacle, as it did with $F=0.5$, but instead begins to steepen and form a breaker. This is an excellent example of a blocking process. In the asymptotic state it is expected that a new upstream fluid level results and a hydraulic jump exists in the obstacle lee. The calculation time is, however, too short to show this new upstream level. We shall return to this question in section 3.3.

Fig. 6 illustrates a supercritical unsteady flow regime. Again we have an initial elevation wave ahead of the obstacle and depression wave in the wake. Unlike the

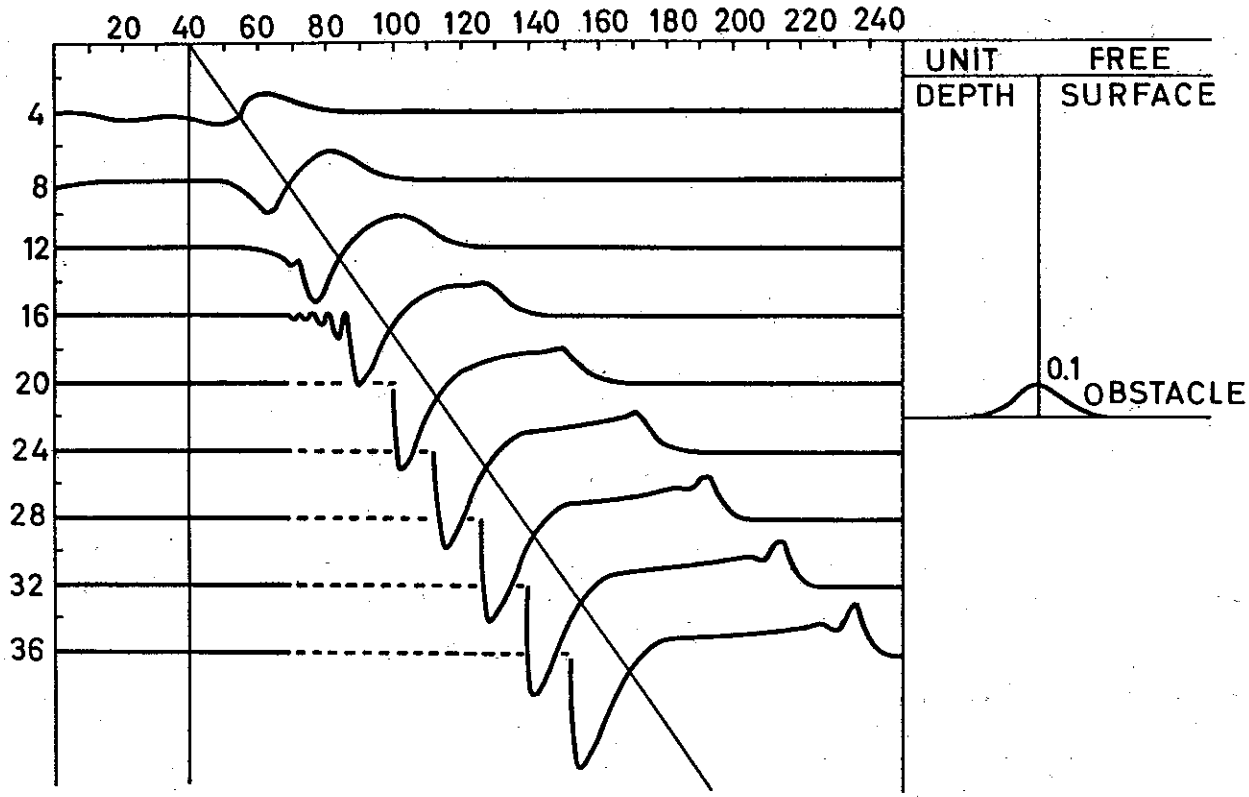

Fig. 5. Numerical results for a Froude number of 0.7 and an obstacle amplitude of 0.1. The grid spacing is 0.2.

high speed case where the elevation wave moved back over the obstacle to give the steady solution, the elevation wave here obtains a large enough amplitude to maintain itself ahead of the obstacle. The inevitable breaking then occurs which leads to the upstream flow shown. Because the numerical integration does not follow accurately the discontinuities, the free surface immediately in front of the obstacle is not adequately described at large times.

The downstream depression wave steepens into a bore and begins to fall behind the moving obstacle. In an asymptotic state a new fluid level, depth less than unity, would appear in the lee. A lee jump is then required to return the fluid level to the original unit depth.

In each of the illustrations it is clear that the numerical oscillations which developed near jumps did not affect the over-all solution. However, if solutions are desired for long times it is necessary to use a numerical method which follows discontinuities and satisfies the normal hydraulic jump conditions across these discontinuities. One possibility is to use characteristic methods but with a moving obstacle this could prove to be rather time consuming.

After completion of the calculations reported here the author discovered that Houghton using a Lax-Wendroff method was investigating the same problem.

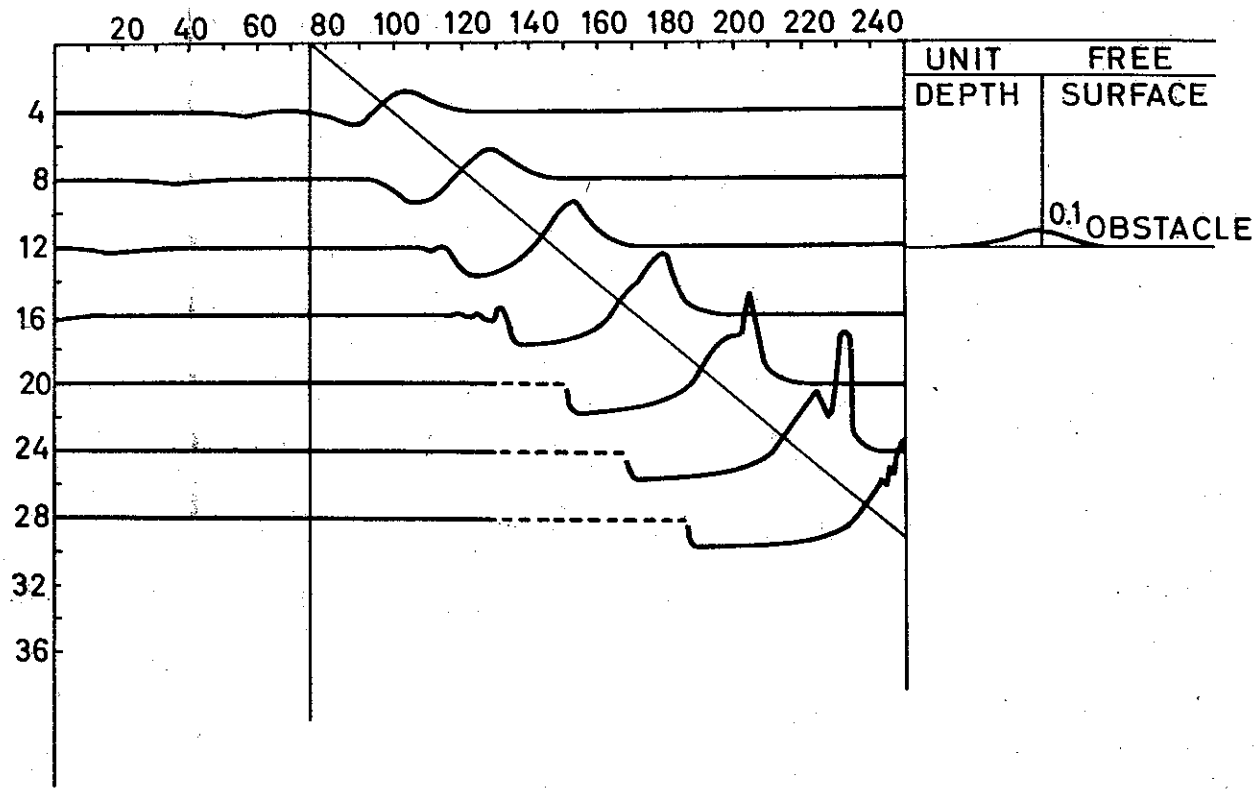

Fig. 6. Numerical results for a Froude number of 1.2 and an obstacle amplitude of 0.1. The grid spacing is 0.2.6.

In Houghton's results numerical oscillations occurring at jumps are damped. The effect of this damping in other parts of the field is currently being investigated.

3.3 The non-steady flow regime. Even in the non-steady flows the free surface shape in the immediate vicinity of the obstacle reaches a steady shape. It follows that the free surface must be described by equations of the form (3.3) and (3.4). The constants of integration K_1 and K_2 are not, however, easily related to the upstream conditions because of the unknown asymptotic state of the upstream conditions.

Some further understanding of the non-steady solutions is obtained if we look at the behavior of the local Froude number. This number is defined relative to a coordinate system moving with the obstacle and based on the actual fluid depth. In Figs. 7a and 7b the local Froude number is shown as a function of time for several positions along the obstacle.

We see from 7a and 7b that at the obstacle crest the local Froude number approaches unity. The dip in the curve in Fig. 7b for large times appears to be a result of numerical instability at the upstream jumps. The asymptotic state before the onset of this instability is clearly indicated. Thus it appears in all cases of unsteady flow that the asymptotic state of motion is such that the local Froude number is unity at the obstacle

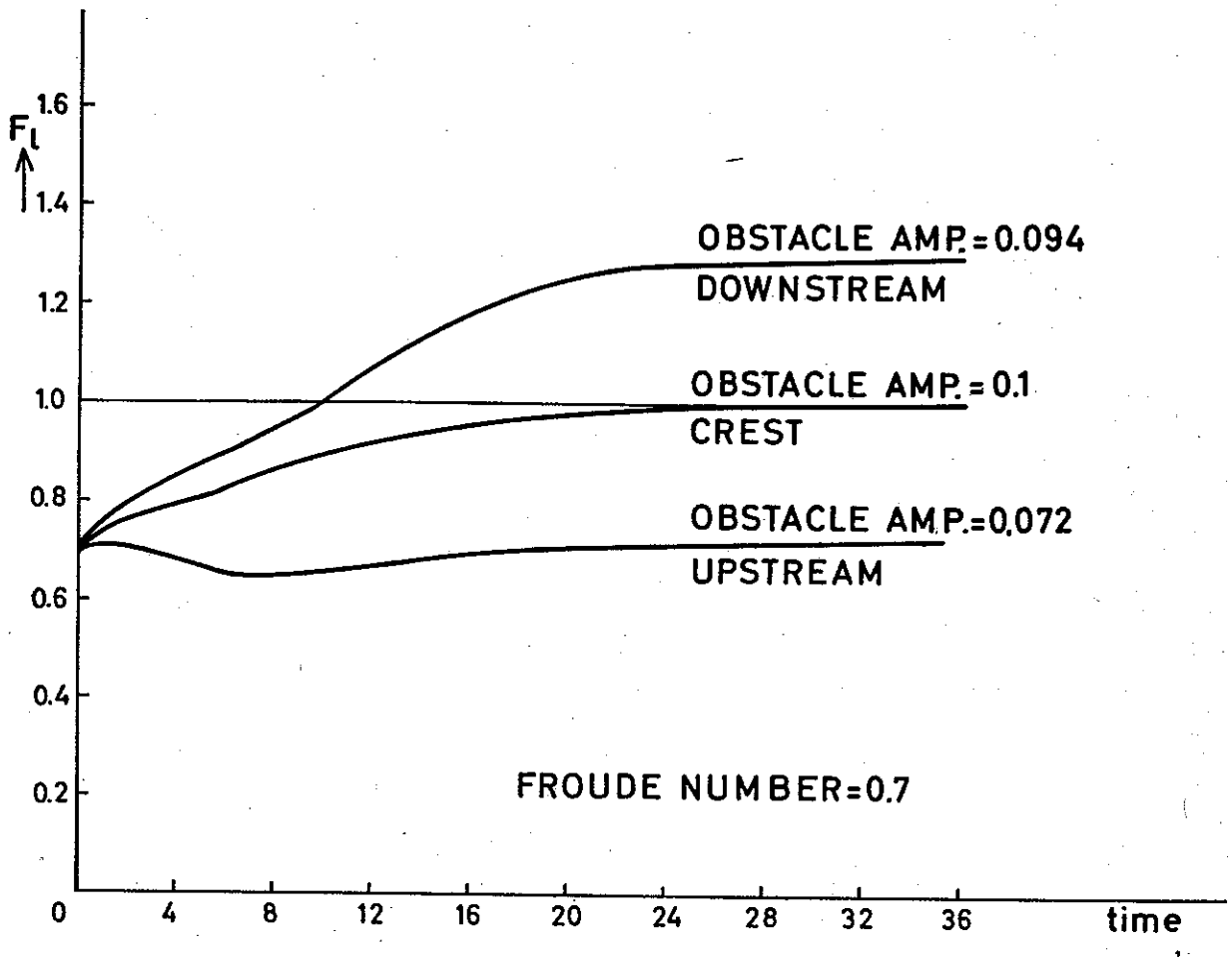

Fig. 7a. Dependence of the local Froude number, F_l, on time for an obstacle speed of $F = 0.7$.

crest. This condition could also be arrived at by intuitive reasoning, for if we examine the experimental and numerical results, we see the non-steady regime is characterized by an asymmetrical free surface shape. The surface is elevated in front of the obstacle and depressed in the lee. Thus hydraulic jumps are required if the fluid is to go from unit depth far ahead of the barrier to a greater depth immediately in front of the barrier, then to a small depth on crossing the obstacle from which it must return to unity some place in the lee. The flow will be subcritical immediately in front of the barrier and supercritical behind the barrier. The transition must occur at the obstacle crest as the local Froude number decreases only with an increasing obstacle amplitude. When looked at from this viewpoint Figs. 7a and 7b show the accuracy of the numerical calculations.

Combining equations (3.3) and (3.4) we find

$$h^3-(K_2-s(x))h^2+\frac{K_1^2}{2}=0. \tag{3.17}$$

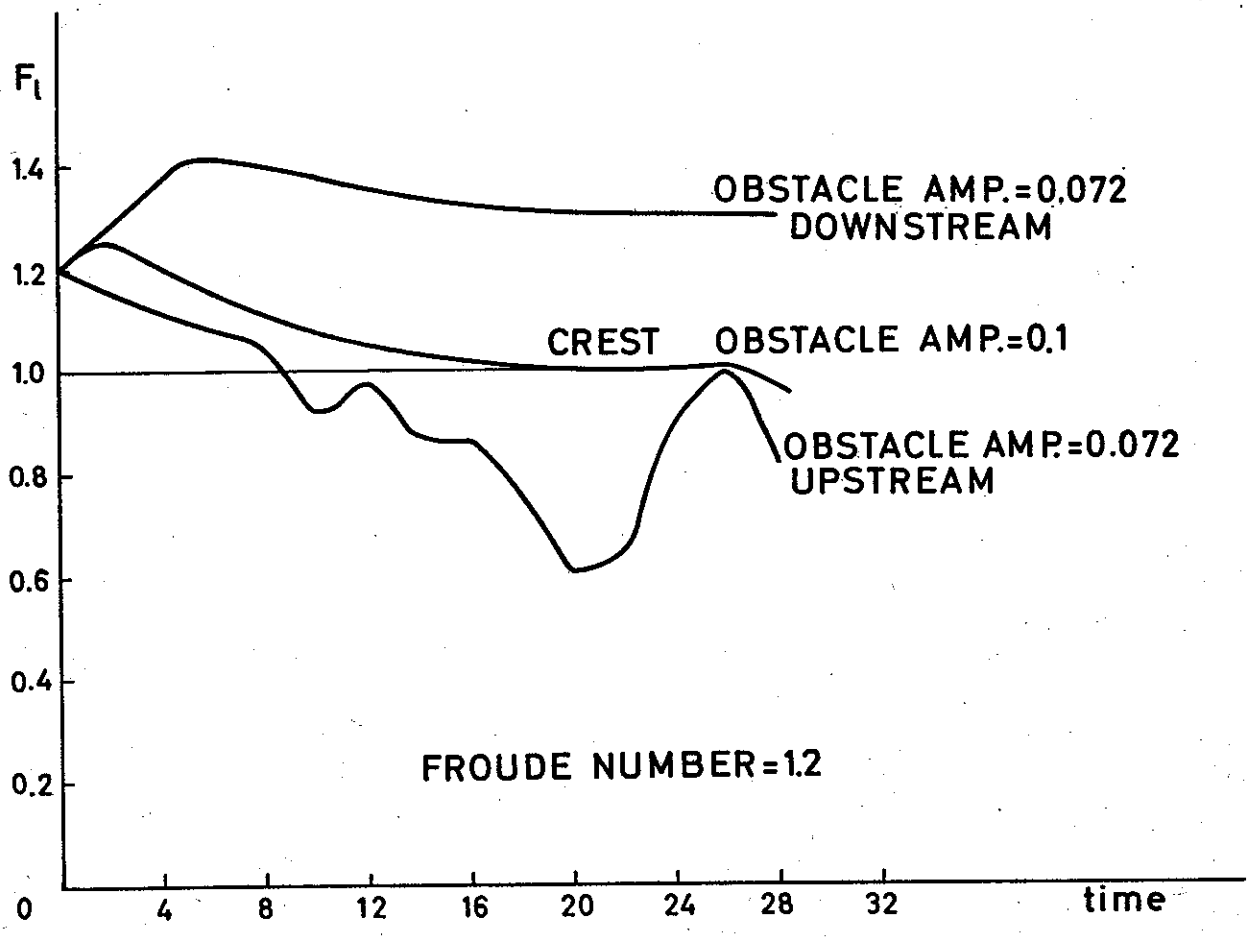

Fig. 7b. Dependence of the local Froude number, F_l, on time for an obstacle speed of $F = 1.2$.

In section 3.1 we show that the condition that the local Froude number be unity is for the cubic (3.17) to possess a double root at the obstacle maximum. This condition is easily found to be

$$K_2 - s_{\max} = \frac{3}{2} K_1^{2/3}. \tag{3.18}$$

and the roots at $s = s_{\max}$ are

$$h_1 = h_2 = K_1^{2/3}, \qquad h_3 = -\tfrac{1}{2} K_1^{2/3}. \tag{3.19}$$

From the definition of the local Froude number it immediately follows that this number is unity at the wave crest. Combining (3.17) and (3.18) we find the free surface is described by

$$h^3 - \left(\frac{3}{2} K_1^{2/3} + s_{\max} - s(x)\right) h^2 + \frac{K_1^2}{2} = 0. \tag{3.20}$$

Physically K_1 is the volume flux over the obstacle. As an upstream bore is equivalent

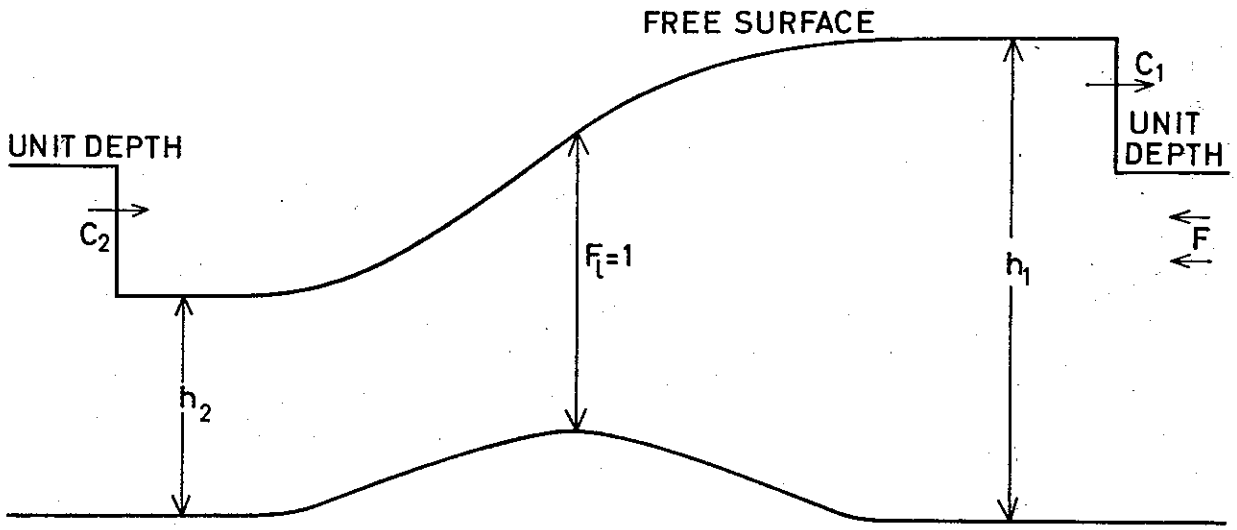

Fig. 8. Illustration of the asymptotic shape of the free surface for flows in the unsteady regime. The unsteadiness is concentrated in the two bores. No particular scale is used in the Figure.

to some of the fluid approaching the obstacle at infinity not reaching the obstacle, it follows that K_1 will be less than F. Thus the only unknown is the actual amount of fluid which crosses the obstacle.

Figs. 7a and 7b, in addition to showing the local Froude number at the obstacle crest, show Froude numbers before and after the crest. The trend in both cases is towards high Froude numbers in the lee. The curve in Fig. 7b for $F=1.2$ shows the effect of unsteadiness in front of the obstacle. This unsteadiness is real for times less than 20 but after that appears to be numerical.

Should the bores move away from the obstacle then we can calculate the value of K_1 as follows. Using the notation illustrated in Fig. 8, we can calculate using classical bore theory the relations between C_1, the speed of the upstream bore relative to the obstacle, C_2, the speed of downstream bore, and the fluid depths before and after the obstacle. These depths are also given by the roots of the cubic (3.20). A final relation between the parameters is obtained from continuity. The fluid crossing the obstacle is the incoming fluid less what does not reach the obstacle because of the upstream bore. These relations are too complicated for analytical solution and no attempt is made in this report to construct the solutions graphically. The equations are 5 relations between 5 variables and thus yield a unique result. It is possible that for some situations the hydraulic jumps will occur over the obstacle. This will complicate the analysis.

4. Lee waves. We have shown in the previous section that a hydrostatic theory possesses almost all the features observed experimentally. In fact the only feature missing from the hydrostatic theory is the development of small amplitude lee waves at low speeds. In a single fluid system the observed lee waves are of very small amplitude and

thus relatively unimportant but in a layered system the amplitude of lee waves can become very large. It is with the problem of lee waves in a layered or even a stratified system in mind that we devote this section to a study of non-linear effects due to a finite obstacle size on the occurrence of lee waves.

For steady flows in a coordinate system moving with the obstacle (2.12) and (2.15) may be integrated to yield

$$(1+\eta-s)U+\frac{1}{3!}(s^3-(1+\eta)^3)U_{xx}-\frac{1}{2!}(s^2-(1+\eta)^2)(Us)_x=F, \tag{4.1}$$

and

$$1+\frac{F^2}{2}=1+\eta+\frac{F^2}{2}+\frac{(1+\eta)^2}{2!}\eta_{xx}+(1+\eta)^2U_x^2+(1+\eta)U(Us)_{xx}+\tfrac{1}{2}(Us)_x^2-(1+\eta)U_x(Us)_x. \tag{4.2}$$

The constants of integration have been evaluated from the upstream flow. Equations (4.1) and (4.2) may be combined if we successively approximate for U in (4.1) obtaining a single equation for U in terms of h. Substituting this value for U into (4.2) we obtain

$$\left\{h^4\left(\frac{h^2}{2}+hs+\frac{s^2}{2}\right)+F^2h\left(-\tfrac{1}{2}s^2-\frac{h^2}{6}-hs\right)\right\}h_{xx}+\left\{-\frac{4}{3}h^2-2hs+s^2\right\}F^2h_x^2+$$

$$+\left\{-\frac{4}{3}h^2-10hs-s^2\right\}F^2h_xs_x+\left\{\frac{h^2}{2}-\frac{13}{3}hs-\frac{1}{6}s^2\right\}F^2s_x^2= \tag{4.3}$$

$$=-h^2\left[h^3-\left(1+\frac{F^2}{2}-s\right)h^2+\frac{F^2}{2}\right]-\left\{h^4\left(\frac{h^2}{2}+hs+\frac{s^2}{2}\right)+\frac{2}{3}F^2h^3\right\}s_{xx}.$$

Equation (4.3) is to be solved with the initial conditions

a) upstream of the obstacle s vanishes and h is unity, and
b) upstream of the obstacle h_x vanishes.

Before considering the numerical solution of (4.3) it is instructive to strip the equation of all of its non-essential features. First we shall linearize the coefficient of h_{xx} and second we neglect the terms h_x^2, h_xs_x, s_x^2. Furthermore we shall assume a very long obstacle and neglect s_{xx}. With these simplifications (4.3) becomes

$$\left(\tfrac{1}{2}-\frac{F^2}{6}\right)h_{xx}=-h^2\left[h^3-\left(1+\frac{F^2}{2}-s\right)h^2+\frac{F^2}{2}\right]. \tag{4.4}$$

The right-hand side of this equation is proportional to the cubic equation (3.5) which occurs in the hydrostatic theory. The qualitative behavior of (4.4) is seen if we examine the cubic shown in Figs. 1a and 1b.

First in a subcritical flow the initial conditions are at the root $h_1=1$ indicated in Fig. 1a. If we now quasi-statically increase the obstacle amplitude we see that the value of the cubic is positive for a fluid of unit depth. It follows from (4.4) that h_{xx} is negative and the fluid depth will begin to curve downward. This curving trend continues until the value of depth is decreased below the root of the cubic whereupon the depth begins to curve upwards. This argument may be continued for further increases in the obstacle size. It is clear that provided three real roots of the cubic exist the solution of (4.4) will tend to follow the largest root of the cubic. Should the obstacle exceed in amplitude the critical size, then for positive h the cubic is positive everywhere and it follows that the fluid depth must decrease until it reaches the only real root of the cubic. This root being negative indicates that no steady flow exists. Thus we see that as the fluid begins to cross the obstacle it follows more or less a hydrostatic flow regime. On the downstream side the fluid depth again increases but now, due to non-hydrostatic effects, a wave train may develop in the lee.

Second in the case of supercritical flow the initial conditions correspond to the root $h_1=1$ in Fig. 1b. Now as the obstacle amplitude is increased the cubic again is positive and consequently h_{xx} is negative. Unlike the subcritical case, now as h decreases the cubic remains positive and the solution of (4.4) will not tend to follow the interesting root of the cubic. Negative values of h are quickly reached. A phase plane analysis of (4.4) would show that $h=1$ is a stable node if the flow is subcritical and an unstable node if the flow is supercritical. If the term involving s_{xx} is included, the above discussion is only slightly modified.

In Fig. 9 we show a set of numerical solutions of (4.3) for the obstacle $s(x) = (0.1)\ \mathrm{sech}^2\ (x/4)$.

The equation was solved numerically by a central difference method with an iterative procedure convergent to at least 1/10000. The obstacle drawn to the same scale as the free surface displacements is shown at the bottom of the Figure. The flow is left to right. Here we see that over the obstacle the fluid tends to follow the hydrostatic prediction, that is, a root of the cubic. In the obstacle lee, wave trains containing waves of very small amplitude are observed. The Froude number of 0.62 was the largest for which solutions could be obtained. All larger Froude numbers led to oscillations about a negative fluid depth.

As the Froude number is increased the displacement of the free surface over the obstacle increases and the amplitude of the lee waves is observed to increase. The term involving s_{xx} has the effect of moving the minimum in the free surface depression behind the obstacle maximum. The critical obstacle size is almost in agreement with the hydrostatic prediction. The departure being due to the inclusion of higher order terms.

The limitations of equation (4.3) may be found if we measure the wavelength of the calculated lee waves. These waves in nature obey the Stokes frequency equation and a measure of the correctness of the over-all solution is the agreement of the wavelength. Since the waves are of very small amplitude, a linearized version of (4.3) may

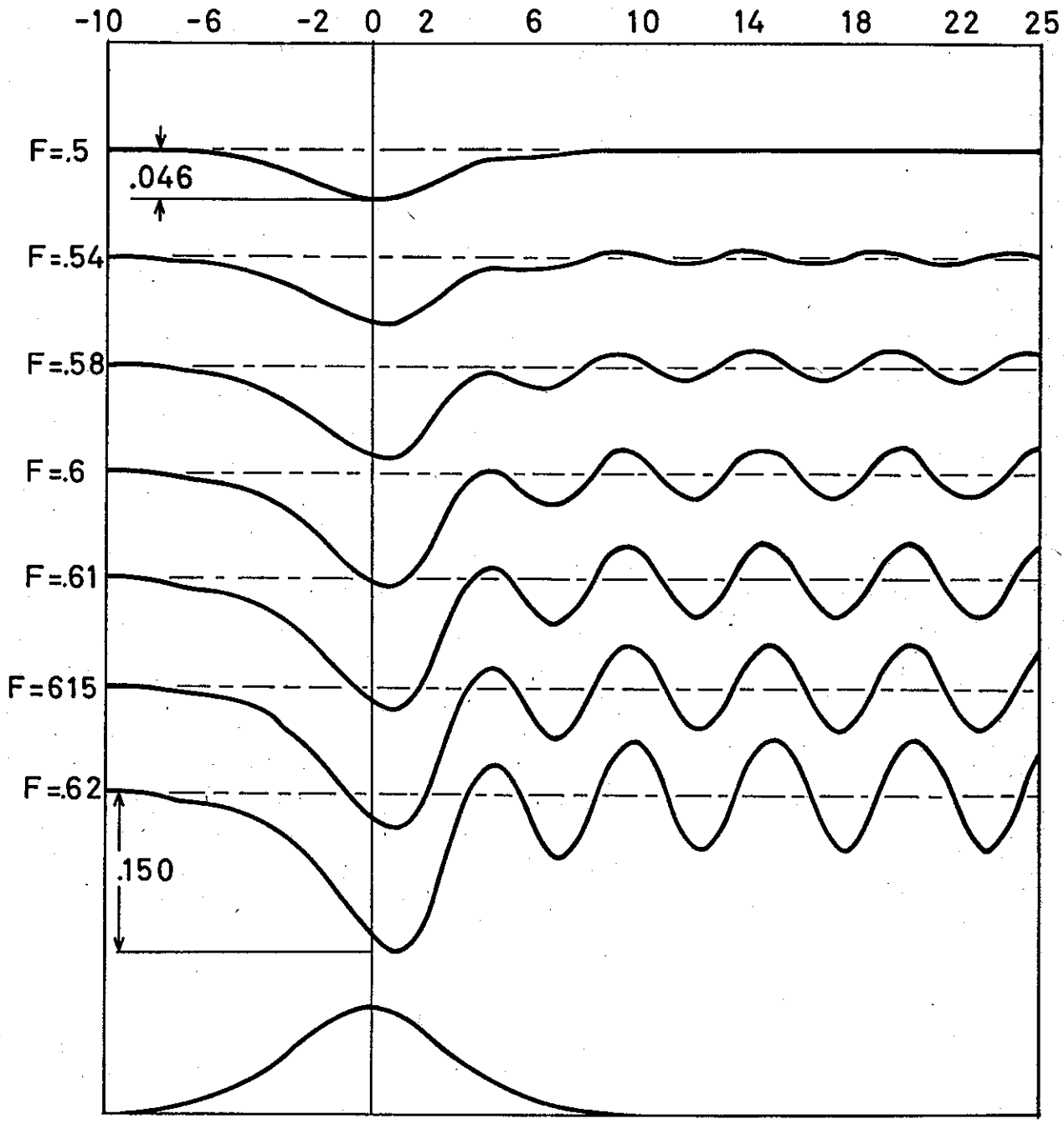

Fig. 9. Wave trains resulting from an obstacle of amplitude 0.1. No steady flow exists for Froude numbers greater than 0.62.

be used for the free waves. If we set $h=1+\omega$ and neglect all quadratic terms, we find

$$\left(\tfrac{1}{2}-\frac{F^2}{6}\right)\omega_{xx}=(F^2-1)\omega\,. \tag{4.5}$$

The obstacle is neglected as we are interested in the free waves. Equation (4.5) has a sinusoidal wave solution with the frequency equation

$$k^2=\frac{6(1-F^2)}{3-F^2}, \tag{4.6}$$

where k is the wave-number. In the derivation of (4.3) we neglected all wave-numbers higher than k^2, thus it is consistent to approximate (4.6) by

$$F^2=1-k^2/3\ . \tag{4.7}$$

It is easily seen that (4.7) contains the leading terms in the expansion in wave-number of the Stokes frequency equation $F^2=\frac{1}{k}\tanh k$.

In Fig. 10 we plot (4.6), (4.7) and the Stokes frequency equation. In all computer runs on (4.3) the wave-length of the waves in the wave trains agreed with (4.6), and consequently we see that the results for the free waves are valid only for Froude numbers near unity. However near the obstacle, the region of major concern, (4.3) is valid for all Froude numbers provided the obstacle is long enough.

This points out one major difficulty which occurs when the Froude number is far from unity. As two scales of motion exist, that of the obstacle and that of the free waves, an approximation scheme based on a long obstacle if extended to the free surface profile can only be valid if the flow is near critical. Yet such an approximation scheme may be used to test for the existence of lee waves at all speeds even though it is known that the wrong wave-lengths are predicted. Strictly, equation (4.3) is valid only for very small obstacles as it is only then that the critical Froude number is near unity.

As the solitary wave approximation procedure may be extended to stratified systems it is interesting to examine the result of such an approximation on (4.3). The solitary wave assumption is equivalent to linearizing the coefficients of h_{xx} and s_{xx}, neglecting first derivative terms and retaining only quadratic terms in ω, $h\equiv 1+\omega$, in the driving term. This results in the equation

$$\left(\tfrac{1}{2}-\frac{F^2}{6}\right)\omega_{xx}=-s-\left(\tfrac{1}{2}+\frac{2}{3}F^2\right)s_{xx}-\omega(1-F^2+4s)+\left(\frac{5}{2}F\ -4\right)\omega^2. \tag{4.8}$$

It is easily demonstrated that with $s=0$ this equation has the solution

$$\omega=a\,\mathrm{sech}^2 bx, \tag{4.9}$$

where

$$b^2=\frac{(F^2-1)}{\left(2-\frac{2}{3}F^2\right)}, \tag{4.10}$$

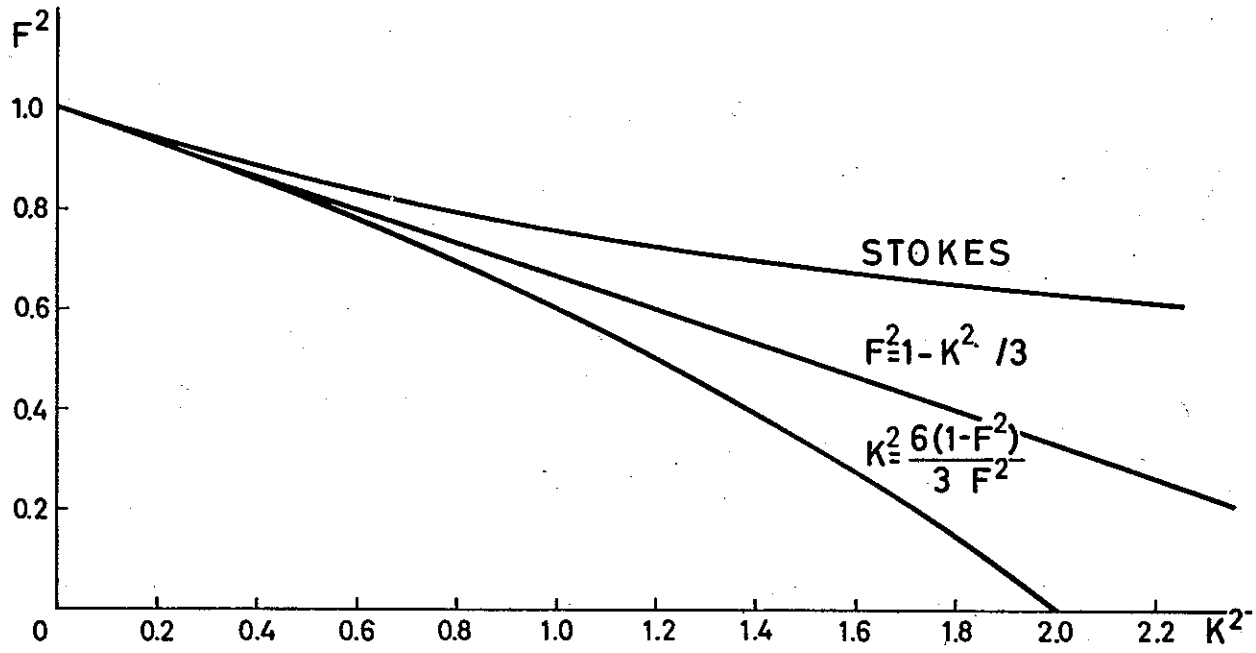

Fig. 10. Diagrams of the three frequency equations discussed in the text.

and

$$a=\frac{3}{2}\frac{(1-F^2)}{\left(\frac{5}{2}F^2-4\right)}. \tag{4.11}$$

Expanding (4.10) and (4.11) in a series in the amplitude we find

$$b^2=\frac{3}{4}a, \tag{4.12}$$

and

$$F^2=1+a, \tag{4.13}$$

the usual solitary wave formula.

With respect to our problem the more interesting feature is the quadratic

$$f(\omega)=\omega^2\left(\frac{5}{2}F^2-4\right)-\omega(1-F^2+4s)-s, \tag{4.14}$$

obtained from the right-hand side of (4.8) if the obstacle curvature is neglected. First let us compare the interesting root of (4.14) with that of (3.5). From (4.14) we find

$$\omega_1=-\frac{F^2s}{(1-F^2)}-\frac{3}{2}\frac{F^2s^2}{(1-F^2)^3}+\cdots, \tag{4.15}$$

and from (3.5) we have

$$h_1-1=\frac{-F^2s}{(1-F^2)}-\frac{3}{2}\frac{F^2s^2}{(1-F^2)^3}+\cdots. \tag{4.16}$$

These two roots are observed to agree to the order of s^2. In comparing the second root of (4.14) with the other positive root of (3.5), agreement is found only in the leading term. Thus a solitary wave approximation is an approximation of the cubic (3.5) by a quadratic.

Furthermore, by comparing the critical obstacle size as predicted by (4.14) with that predicted by (3.7) both equations are found to have the expansion

$$F_c^2=1\pm(6s_c)^{\frac{1}{2}}. \tag{4.17}$$

Thus for small obstacle amplitudes we predict the correct critical obstacle amplitude. Consequently the use of a solitary wave approximation scheme is justified if the flow is near critical.

5. Concluding remarks. In this discussion we have been concerned only with the flow of a perfect fluid over a submerged barrier. LONG (1954) has observed that layered systems behave very similarly to a single fluid system. Thus the ideas set forth here are easily translated to a layered system even though an actual analysis is much more complex. For example in a two-layered system the analogy to (3.3) is a sixth order equation. For a n-layered fluid system the equation is of order $3n$. Equations of such large order are very difficult to handle and thus we restricted ourselves to a simple system in which results are more easily interpreted. From the experiments it appears that the only new phenomenon introduced in a layered system is the possibility of hydraulic jumps down.

The results of this work are twofold. First it has been shown how the non-linear development of free waves in the initial value problem influences the asymptotic state of the system. If a shock-free asymptotic state exists, it agrees with the steady prediction. Second we have shown how the existence of lee waves depends on the obstacle size. Lee waves are found for subcritical flow and only then if the hydrostatic theory predicts a steady flow.

One feature of the experimental observations which is not explained is the development of undular hydraulic jumps. Such phenomena which occurred only in subcritical flow and for obstacles slightly larger than the critical size should be contained in the full time-dependent equations. Unfortunately no stable method for numerically integrating these equations has been found. It is not expected that the undular hydraulic jumps can be obtained from a steady analysis.

ACKNOWLEDGEMENTS

I thank Professor Arnt Eliassen for his many helpful comments and for making available the facilities at the University of Oslo. This work was performed while I was a National Science Foundation Post-doctoral Fellow.

REFERENCES

FRIEDRICHS, K. O., 1948: On the derivation of the shallow water theory. *Comm. Appl. Math.* **1**, 81–85.

KELLER, JOSEPH B., 1948: The solitary wave and periodic waves in shallow water. *Comm. Appl. Math.* **1**, 323–339.

LAMB, HORACE, 1932: *Hydronamics*, 6th ed. XV+738 pp. Cambridge: Cambridge University Press, New York: Dover Publications, 1945, 423–427.

LONG, R. R., 1954: Some aspects of the flow of stratified fluids II. Experiments with a two-fluid system. *Tellus*, **6**, 97–115.

— 1955: Some aspects of the flow of stratified fluids III. Continuous density gradients. *Tellus*, **7**, 341–257.

— 1964: The initial value problem for long waves of finite amplitude. *J. Fluid Mech.*, **20**, 161–171.

STOKER, J. J., 1957: *Water waves. The mathematical theory with applications.* XXVIII+567 pp. New York: Interscience.

WEHAUSEN, J. V. and E. V. LAITONE, 1960: *Surface waves.* Handbuch der Physik, Springer Verlag, 446–778.

YIH, CHIA-SHUN, 1965: *Dynamics of nonhomogeneous fluids.* New York: Macmillan Company 306 pp.

Avhandlinger som ønskes opptatt i «Geofysiske Publikasjoner», må fremlegges i Videnskaps-Akademiet av et sakkyndig medlem.

Vol. XXII.

No. 1. L. Harang and K. Malmjord: Drift measurements of the E-layer at Kjeller and Tromsø during the international geophysical year 1957—58. 1960.
» 2. Leiv Harang and Anders Omholt: Luminosity curves of high aurorae. 1960.
» 3. Arnt Eliassen and Enok Palm: On the transler of energy in stationary mountain waves. 1961.
» 4. Yngvar Gotaas: Mother of pearl clouds over Southern Norway, February 21, 1959. 1961.
» 5. H. Økland: An experiment in numeral integration of the barotropic equation by a quasi-Lagrangian method. 1962.
» 6. L. Vegard: Auroral investigations during the winter seasons 1957/58—1959/60 and their bearing on solar terrestrial relationships. 1961.
» 7. Gunnvald Bøyum: A study of evaporation and heat exchange between the sea surface and the atmosphere. 1962.

Vol. XXIII.

No. 1. Bernt Mæhlum: The sporadic E auroral zone. 1962.
» 2. Bernt Mæhlum: Small scale structure and drift in the sporadic E layer as observed in the auroral zone. 1962.
» 3. L. Harang and K. Malmjord: Determination of drift movements of the ionosphere at high latitudes from radio star scintillations. 1962.
» 4. Eyvind Riis: The stability of Couette-flow in non-stratified and stratified viscous fluids. 1962.
» 5. E. Frogner: Temperature changes on a large scale in the arctic winter stratosphere and their probable effects on the tropospheric circulation. 1962.
» 6. Odd H. Sælen: Studies in the Norwegian Atlantic Current. Part II: Investigations during the years 1954—59 in an area west of Stad. 1963.

Vol. XXIV.

In memory of Vilhelm Bjerknes on the 100th anniversary of his birth. 1962.

Vol. XXV.

No. 1. Kaare Pedersen: On the quantitative precipitation forecasting with a quasi-geostrophic model. 1963.
» 2. Peter Thrane: Perturbations in a baroclinic model atmosphere. 1963.
» 3. Eigil Hesstvedt: On the water vapor content in the high atmosphere. 1964.
» 4. Torbjørn Ellingsen: On periodic motions of an ideal fluid with an elastic boundary. 1964.
» 5. Jonas Ekman Fjeldstad: Internal waves of tidal origin. 1964.
» 6. A. Eftestøl and A. Omholt: Studies on the excitation of N_2 and N_2^+ band sin aurora. 1965.

Vol. XXVI.

No. 1. Eigil Hesstvedt: Some characteristics of the oxygen-hydrogen atmosphere. 1965.
» 2. William Blumen: A random model of momentum flux by mountain waves. 1965.
» 3. K. M. Storetvedt: Remanent magnetization of some dolerite intrusions in the Egersund Area, Southern Norway. 1966.
» 4. Martin Mork: The generation of surface waves by wind and their propagation from a storm area. 1966.
» 5. Jack Nordø: The vertical structure of the atmosphere. 1965.
» 6. Alv Egeland and Anders Omholt: Carl Størmer's height measurements of aurora. 1966.
» 7. Gunnvald Bøyum: The energy exchange between sea and atmosphere at ocean weather stations M, I and A. 1966.
» 8. Torbjørn Ellingsen and Enok Palm: The energy transfer from submarine seismic waves to the ocean. 1966.
» 9. Torkild Carstens: Experiments with supercooling and ice formation in flowing water. 1966.
» 10. Jørgen Holmboe: On the instability of stratified shear flow. 1966.
» 11. Lawrence H. Larsen: Flow over obstacles of finite amplitude. 1966.

A.s John Griegs Boktrykkeri